Participation of Two Carboxyl Groups in Phosphodiester Hydrolysis. 2. A Kinetic, Isotopic, and ^{31}P NMR Study of the Hydrolysis of a Phosphodiester with Carboxyl Groups Fixed in an Attack Conformation

Thomas C. Bruice,* Andrei Blaskó, Ramesh D. Arasasingham, and Jang-Seob Kim

Contribution from the Department of Chemistry, University of California, Santa Barbara, California 93106

Received June 16, 1995[⊗]

Abstract: The phosphodiesters of 4,4′-methylenebis(3-hydroxy-2-naphthoic acid) (**4**) and 3-carboxy-2,2′-dihydroxydiphenylmethane (**5**) are constrained into a cyclic structure such that the oxygens of the two *o*-carboxy groups of **4** and the single *o*-carboxy group of **5** have restricted stereospecific positions with an *o*-CO_2^- oxygen to phosphorus distance of 3.7 Å. In the hydrolysis of **4**, ^{31}P NMR and HPLC data show the existence of an intermediate cyclic acyl phosphate in the *g,g* conformation. The ^{18}O isotopic effects on ^{31}P chemical shifts show incorporation of two ^{18}O atoms in the product H_3PO_4. This observation is consistent with intramolecular *o*-CO_2^- nucleophilic attack on phosphorus to provide an acyl phosphate intermediate which undergoes hydrolytic cleavage by $HO^-/H^{18}O^-$ attack on phosphorus {one ^{18}O incorporation} to provide a phosphate monoester which also undergoes hydrolysis with a second ^{18}O incorporation on phosphorus. For hydrolysis of **4**, the pH *vs* log k_{obsd} profile, the values of the deuterium solvent kinetic isotope effect, and the activation entropy accord a mechanism which involves intramolecular attack of *o*-CO_2^- on the phosphate phosphorus assisted by the *o*-CO_2H as a general acid catalyst. The latter can involve *o*-CO_2H hydrogen bonding to the -(PO_2^-)- oxygen(s) and/or leaving phenolic oxygen. At neutrality, **4** hydrolyzes *ca.* 10^4 fold faster than **5** which only has one *o*-carboxy group and 10^8-10^9-fold faster than diphenyl phosphate.

Introduction

Possibly due to the importance of the phosphodiester linkages of DNA and RNA, there has been considerable interest in the mechanisms of phosphodiester hydrolysis[1,2] and the bifunctional acceleration of phosphorolytic reactions (Thatcher and Kluger propose that these reactions be defined more correctly as metaphosphatylation processes[2]). In the paper preceding the present study[3] in this issue of the journal, we describe a computational and experimental investigation of the hydrolysis of bis(2-carboxyphenyl) phosphate (**1**). Originally, it had been reported that hydrolysis of **1**, due to intramolecular nucleophilic

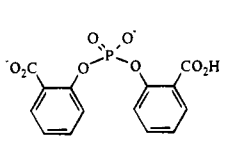

1

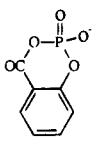

2

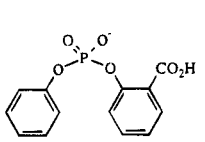

3

attack by *o*-CO_2^- (to provide **2**), received a surprisingly small rate enhancement over the hydrolysis of **3** by the presence of the *o*-CO_2H.[4] Such a small rate enhancement by *o*-CO_2H general acid participation appeared odd because intramolecular hydrogen bonding would be expected to be of kinetic importance. This is so regardless of whether the rate-determining step was nucleophilic attack on P {hydrogen bonding to -(PO_2^-)-} or departure of the ^-O-Ar leaving group.[5-8] This consideration led us to undertake semiempirical calculations to determine the probability of formation of ground state conformations in which *o*-CO_2^- and *o*-CO_2H are in position to attack P and act as general acid catalyst, respectively. Several such conformations were identified as being predominant. From this we conclude that the role of the second carboxyl in the hydrolysis of **1** is not understood.

In this paper we report our study of the hydrolysis of **4**. In our choice of structure **4** we had in mind the investigation of a model in which the positions of the carboxyl functions were predetermined in space. In **4** the *o*-CO_2H is held in position to interact with both -(PO_2^-)- and the ^-O-Ar departing moiety such that neighboring *o*-CO_2H catalysis is allowed regardless weather the critical transition state involves *o*-CO_2^- attack or departure of the leaving group. Structure **4** represents the phosphodiester of pamoic acid {4,4′-methylenebis(3-hydroxy-2-naphthoic acid)}. In order to comprehend the kinetic importance of the *o*-CO_2H facilitation of *o*-CO_2^- attack on P, we compare the hydrolysis of **4** to the hydrolysis of the phosphodiesters of 3-carboxy-2,2′-dihydroxydiphenylmethane (**5**) and bis-(2-dihydroxyphenyl)methane (**6**).

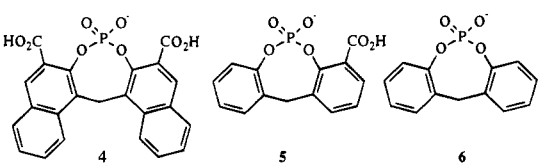

4 **5** **6**

Results

NMR Experiments. The ^{31}P NMR spectrum of **4** was recorded in H_2O/DMSO-d_6 4:1 (v/v). The major signal was

[⊗] Abstract published in *Advance ACS Abstracts,* December 1, 1995.

(1) Gerlt, J. A. In *Nucleases,* 2nd ed.; Linn, S. M., Lloyd, R. S., Roberts, R. J., Eds.; Cold Spring Harbor Laboratory Press: New York, 1993; series title, Cold Spring Harbor monograph series, Vol. 25, Chapter 1.

(2) Thatcher, G. R.; Kluger, R. *Adv. Phys. Org. Chem.* **1989**, *25*, 99.

(3) Bruice, T. C.; Blaskó, A.; Petyak, M. *J. Am. Chem. Soc.* **1995**, *117*, 12064.

(4) Abel, K. W. Y.; Kirby, A. J. *J. Chem. Soc., Perkin Trans. 2*, **1983**, 1171.

(5) Dempsy, R. O.; Bruice, T. C. *J. Am. Chem. Soc.* **1994**, *116*, 4511.

0002-7863/95/1517-12070$09.00/0

Scheme 1

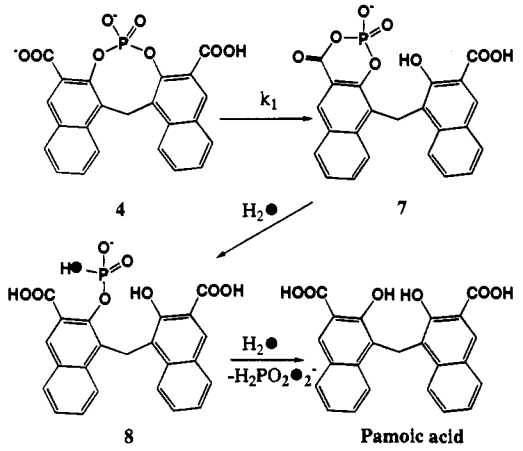

observed at −8.45 ppm, and a minor signal was observed at −11.18 ppm while two very small signals were at −3.22 ppm and −0.66 ppm. The major signal at −8.45 ppm was assigned to the diester **4** and is consistent with the chemical shifts of phosphodiesters in the *g,g* conformation.[9] Acyclic phosphodiesters usually have the ^{31}P chemical shifts below −1 ppm, and δ_P is strongly governed by the bond and the torsional angle effects. Torsional effects alone serve to explain 2−3 ppm upfield shift in phosphodiesters.[10] We assigned the resonance at −11.18 ppm (Figure S1, supporting information) to the cyclic six-membered-ring acyl phosphate (**7**, Scheme 1) because the signal at −11.18 ppm forms and decreases slowly while the signal for **4** at −8.45 ppm disappears in a first-order process. Six-membered cyclic phosphates have ^{31}P chemical shifts in the −4 to −14 ppm region.[9,11,12] A pentacoordinate intermediate is excluded as that with $\delta = -11.18$ ppm because pentacoordinate phosphorus compounds containing five oxygens around phosphorus are found to have chemical shifts between −30 and −90 ppm.[13] Also, pentacoordinate intermediates of a phosphodiester are less stable (as compared to that of a triester).[14] As the signal of the acyl phosphate at −11.18 ppm decreases the signal at −3.22 ppm increases and decreases, to provide the signal at −0.66 ppm. The small, broad signal at −3.22 ppm belongs to the monoester. This signal is essentially identical to that for salicyl phosphate monoester.[3] The signal at −0.66 ppm was the only signal present at the end of the reaction, and it is identical to that for $H_2PO_4^-$.

In the ^1H NMR of **4** {0.1 M formate buffer; 20% DMSO-d_6/D_2O (v/v); pD = 8.4} the CH_2 signal of **4** appears at 5.076 ppm (Figure S2, supporting information). Two additional methylene signals were seen at 5.152 and 5.135 ppm accounting for the CH_2 protons of the intermediates cyclic acyl phosphate and the monophosphate. The CH_2 protons of pamoic acid resonate at 4.994 ppm. As expected, two sets of nonequivalent aromatic resonances were seen shifted at lower frequencies from those of the starting diester **5** and pamoic acid (data not shown).

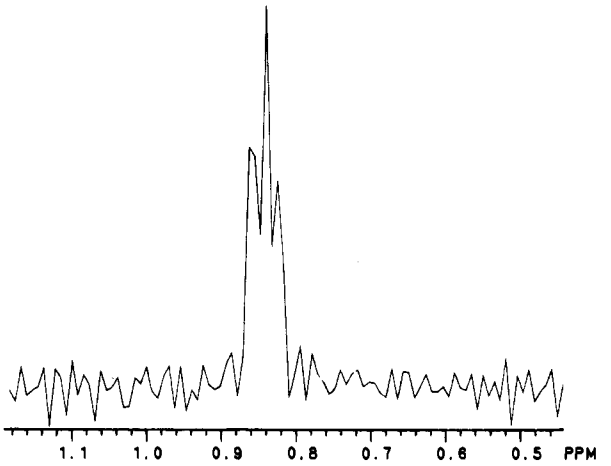

Figure 1. Influence of the ^{18}O incorporation in H_3PO_4, as the reaction product in the hydrolysis of **4**, on the ^{31}P chemical shift. The three ^{31}P signals correspond to H_3PO_4 with no ^{18}O, one ^{18}O, and two ^{18}O atoms incorporated, respectively.

Observation of ^{18}O incorporation by following the ^{31}P chemical shifts in the hydrolysis of **4** was performed in D_2O/$H_2{}^{18}O$ at 25 °C (Experimental Section). For a P−O single bond, the ^{18}O-induced chemical shift per ^{18}O bonded to phosphorus (*S* value) is 0.015−0.025 ppm.[15,16] The final ^{31}P spectrum (Figure 1) is that of phosphoric acid (see Experimental Section). The ^{31}P signal at around 0 ppm contains three peaks distanced by 0.023 and 0.015 ppm, respectively, showing incorporation of both one and two ^{18}O atoms in the phosphoric acid product. The ^{31}P spectrum remained unchanged after 1 week, showing that no exchange phenomena were present under our experimental conditions. Exchange of ^{18}O at H_3PO_4 is slow, $k \approx 10^{-6}$ s^{-1} at 100 °C,[17] comparable to exchange rates of carboxyl oxygens of aliphatic acids[18] with some exceptions.[19]

For the ^{13}C chemical shifts of the carboxyl carbons containing ^{18}O isotopes, a value of $\Delta\delta = 0.02-0.03$ ppm is usually common.[20] The ^{13}C spectrum of the pamoic acid product shows no ^{18}O incorporation, evidenced by a single sharp ^{13}C carboxyl peak at 178.09 ppm. The chemical shift difference between the carbonyl resonances of authentic pamoic acid and product obtained in 50% ^{18}O-enriched water was $\Delta\delta = -0.005$ ppm!

Kinetic Studies. The HPLC separations for the hydrolysis of **4** were performed in order to characterize the reaction intermediates and to determine whether the reaction can be followed by UV−vis spectroscopy. For these experiments we used a reverse phase column in the pH range of 2.0−7.7 and a diode array UV−vis detector (Experimental Section). The reaction mixture was incubated at 40 °C, samples were eluted at room temperature, and the separation was followed at 290

(6) Westheimer, F. H. In *Phosphorus Chemistry, Developments in American Science*; Walsh, E. N., Griffith, E. J., Parry, R. W., Quin, L. D., Eds.; ACS Symposium Series; American Chemical Society: Washington, DC, 1992.
(7) Dalby, K. N.; Holifelder, F.; Kirby, A. J. *J. Chem. Soc., Chem. Commun.* **1992**, 1770.
(8) Khan, S. A.; Kirby, A. J.; Wakselman, M. *J. Chem. Soc. B* **1970**, 1182.
(9) Gorenstein, D. G. In *Phosphorus-31 NMR*; David G. Gorenstein, Ed.; Academic Press: New York, 1984; pp 7−36.
(10) Gorenstein, D. G.; Kar, D. *Biochem. Biophys. Res. Commun.* **1975**, *65*, 1073.
(11) Gallagher, M. J. In *Phosphorus-31 NMR Spectroscopy in Stereochemical Analysis*; Verkade, J. G., Quin, L. D., Eds.; VCH; Deerfield Beach, FL, 1987; p 298.
(12) Munoz, A.; Gallagher, M.; Klaebe, A.; Wolf, R. *Tetrahedron Lett.* **1976**, *9*, 673.
(13) Tebby, J. C., ref 11, p 33.
(14) Bromilow, R. H.; Khan, S. A.; Kirby, A. J. *J. Chem. Soc. B* **1971**, 1091.
(15) Von der Saal, W.; Villafranca, J. J. *Bioorg. Chem.* **1986**, *14*, 28.
(16) Tsai, M.-D., ref 9, p 178.
(17) Bunton, C. A.; Llewellyn, D. R.; Vernon, C. A.; Welch, V. A. *J. Chem. Soc.* **1961**, 1636.
(18) Chon, M.; Urey, H. C. *J. Am. Chem. Soc.* **1938**, *60*, 679.
(19) In the case of phosphoenolpyruvate, in acidic solution and at 98 °C phosphoenolpyruvate exchanges its phosphoryl oxygens with a rate constant of 0.005 and 0.01 s^{-1} at pH 2.0 and 1.1, respectively ($t_{1/2}$ = 2−70 min) (O'Neal, C. C.; Bild, G. S.; Smith L. T. *Biochemistry* **1983**, *22*, 611). In this case the exchange occurs by the formation of an intermediate cyclic phosphate or a transient acyl phosphate which reverts to the initial phosphoenolpyruvate (the cyclic acyl phosphate is formed with a rate constant of 0.027 s^{-1} at 98 °C and 1 M HCl).
(20) O'Leary, M. H.; Hermes, J. D. *Anal. Biochem.* **1987**, *162*, 358.

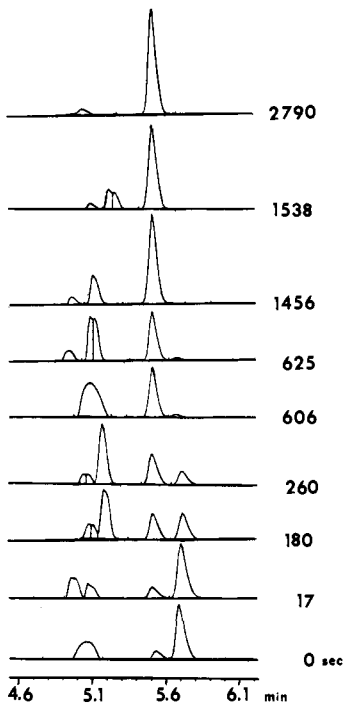

Figure 2. HPLC stacked plot of the hydrolysis of **4** 2.3×10^{-5} M in 0.1 M acetate buffer pH 4.5 at 40 °C at the indicated reaction times.

and 320 nm. Under the reaction conditions, we saw elution of a composite peak at a retention time of 5.1 min. The product pamoic acid eluted at 5.5 min, while the third peak eluting at 5.7 min belongs to the starting ester **4**. With time the peak at 5.7 min retention time decreases and the peak at 5.1 min increases and then gives way to the peak of pamoic acid (Figure 2). The UV−vis spectra of the substrate, intermediates, and product are shown in Figure S3, supporting information. We could not individually follow the reaction intermediates (t_R 5.1 min) due to their poor separation (see Experimental Section). From the NMR experiments (*vide supra*) the composition of the HPLC composite peak must consist of the cyclic six-membered-ring acyl phosphate and the monophosphate ester of pamoic acid.

HPLC kinetic simulations were performed for the sequential first-order system A → B → C, with rate constants k_1 and k_2 (Experimental Section). The experimental points for the changes in integrated areas of A, B, and C {where A is **4**, B is **7**, and C is pamoic acid (Scheme 1)} with time were computer fit to eq 1 in order to obtain the best fit values of k_1 and k_2 (the

$$[A] = A_0 e^{-k_1 t}$$

$$[B] = B_0 e^{-k_2 t} + \frac{k_1 A_0 (e^{-k_1 t} - e^{-k_2 t})}{k_2 - k_1} \qquad (1)$$

$$[C] = A_0\left[1 - e^{-k_1 t} - \frac{k_1 (e^{-k_1 t} - e^{-k_2 t})}{k_2 - k_1}\right] + B_0(1 - e^{-k_2 t})$$

composite peak B contains both intermediates). The k_1 and k_2 values determined at several pH values are provided in Table 1. The HPLC (and ^{31}P NMR) data show a rapid formation of the cyclic acyl phosphate **7** from **4** which breaks down to the monoester **8** and 4,4′-methylenebis(3-hydroxy-2-naphthoic acid) (pamoic acid) in a slow process. A plot of log k_1 *vs* pH follows a bell-shaped curve similar to that obtained by using conventional UV−vis spectroscopy (*vide infra*) at 50 °C (Figure 3 and Table 1). What follows is a detailed study using UV−vis spectroscopy.

Table 1. Values of the Individual Rate Constants[a,b] for the Hydrolysis of **4** at 40 °C (μ = 1.0 with KCl)

pH	buffer	log k_1	log k_2
2.0	HCl	−5.68	−5.66
4.5	acetate 0.05 M	−3.60	−4.20
5.5	acetate 0.05 M	−5.07	−4.80
6.5	phosphate 0.05 M	−5.54	−4.72
7.5	phosphate 0.05 M	−6.30	−3.84

[a] Determined by HPLC at 2.3×10^{-5} M **4** for a A → (k_1) B → (k_2) C system. [b] k_1 and k_2 in s^{-1}.

Table 2. Values of Equilibrium and Rate Constants Determined as Kinetically Apparent Constants and *via* Spectrophotometric Titration (50 °C and μ = 1.0 with KCl)

	values of determined constants[a,b]			
compound	pK_{a1}	pK_{a2}	k_p	$k_q \approx k_r$
4 in H_2O[c]	3.35	4.14	1.8×10^{-3}	
4 in D_2O[c]	3.27	4.97	9.6×10^{-4}	
5 in H_2O	4.34[d]			3.4×10^{-8}

[a] For phosphodiester 4, pK_{a1} and pK_{a2} are defined in Scheme 2, and for phosphodiester 5, pK_{a1} is defined in Scheme 3. [b] Units in mol and s. [c] Kinetically apparent constants obtained by fitting of eq 2 to experimental data points. [d] Determined by spectrophotometric titration.

Use of UV−vis Spectroscopy To Follow the Kinetics of the Hydrolysis of 4, 5, and 6. Reactions were followed at constant values of pH between pH 2 and 8, where the phosphate ester moiety exists primarily as the monoanion {−O−(PO_2^-)−O−}. Reactions were followed by monitoring the appearance of pamoic acid at 250 nm, 3-carboxy-2,2′-dihydroxydiphenylmethane at 300 nm, or bis(2-hydroxyphenyl)methane at 277 nm and their anions, under pseudo-first order conditions at 50 °C and ionic strength 1.0 with KCl. The kinetic runs were initiated by the addition of 50 μL of freshly prepared aqueous (**4** and **5**) or methanolic (**6**) solutions of the diester to the appropriate buffer (3.0 mL). Final concentrations of esters were *ca.* 2×10^{-4} M.

pH Dependence of the Hydrolysis of 4. All reactions of **4** followed the first-order rate law to completion. Timed repetitive scans from 200 to 450 nm demonstrated clean isosbestic points (the positions depending on pH). Below pH 1 and above pH 7, **4** was quite stable to hydrolysis.

Figure 3 shows the plot of the log of the pseudo-first-order rate constants (k_{obsd}) for the hydrolysis of **4** *vs* pH at 50 °C (μ = 1.0 with KCl). The experimental points were fit to eq 2 (standard error = 3.7×10^{-2}), where a_H is the hydrogen ion activity measured at 50 °C. The values of the constants k_p,

$$k_{obsd} = \frac{k_p K_{a1}' a_H}{(K_{a1}' K_{a2}' + K_{a1}' a_H + a_H^2)} \qquad (2)$$

K_{a1}', and K_{a2}' (Schemes 2 and 3) required to fit the experimental rate constants to eq 2 are recorded in Table 2. Values of K_{a1}' and K_{a2}' are kinetically apparent constants. The thermodynamic values for K_{a1} and K_{a2} could not be determined by titration because of the hydrolytic liability of **4**.

Deuterium solvent kinetic isotope effects for the hydrolysis of 4 were determined under an N_2 atmosphere at 50 °C. Progress of reactions at various pD values in D_2O was followed to completion under the same conditions as the reactions in H_2O at constant pH. The final spectra were of 4,4′-methylenebis-

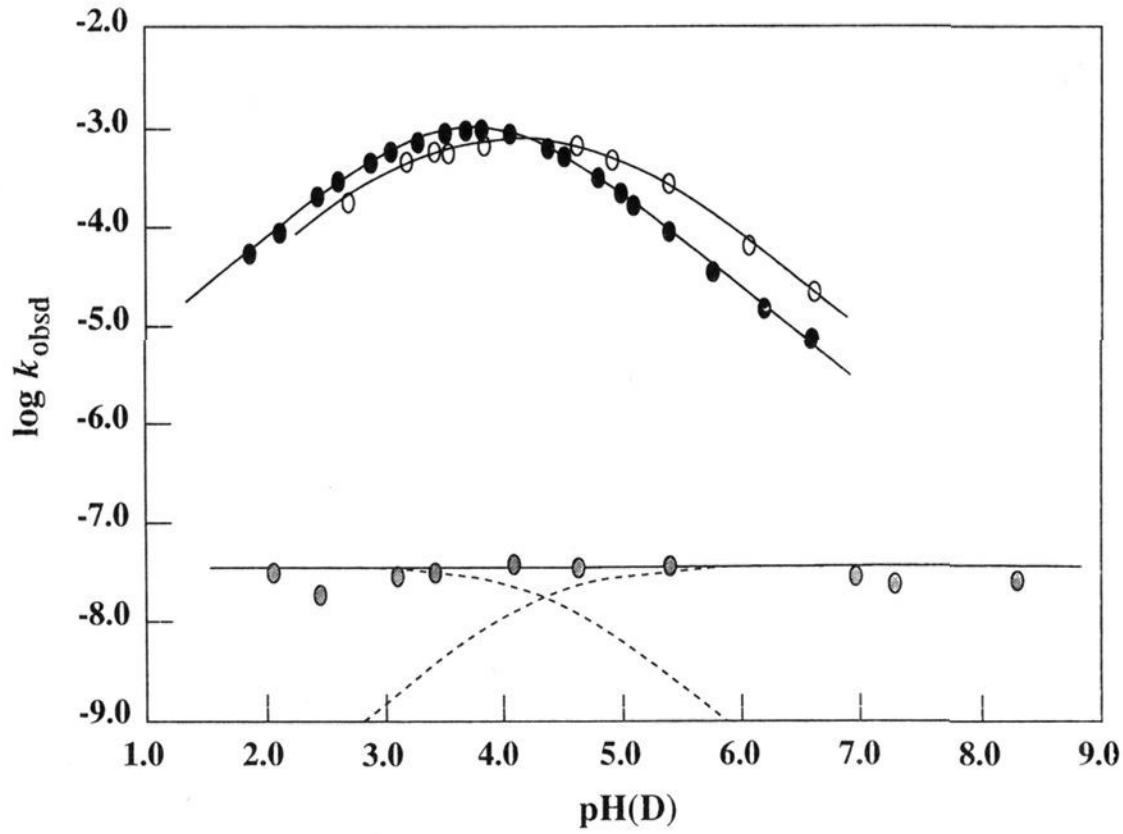

Figure 3. Dependence of the pseudo-first-order rate constants (k_{obsd}) for the hydrolysis of **4** and **5** on acidity {50 °C and ionic strength 1.0 with KCl}. Bell-shaped plots of log k_{obs} *vs* pH(D) for hydrolysis of **4** in H_2O (closed circles) and **4** in D_2O (open circles) and the pH independence of log k_{obs} *vs* pH for hydrolysis of **5** in H_2O (hatched circles). The curves for the hydrolysis of **4** were computer-generated by iteratively fitting the experimental points to eq 2. The values of constants that provided the optimal fits are provided in Table 2. The pH independence of the reaction of **5** arises by addition of the contributions of proton ionized and un-ionized species as shown by the dashed lines (eq 7).

Scheme 2

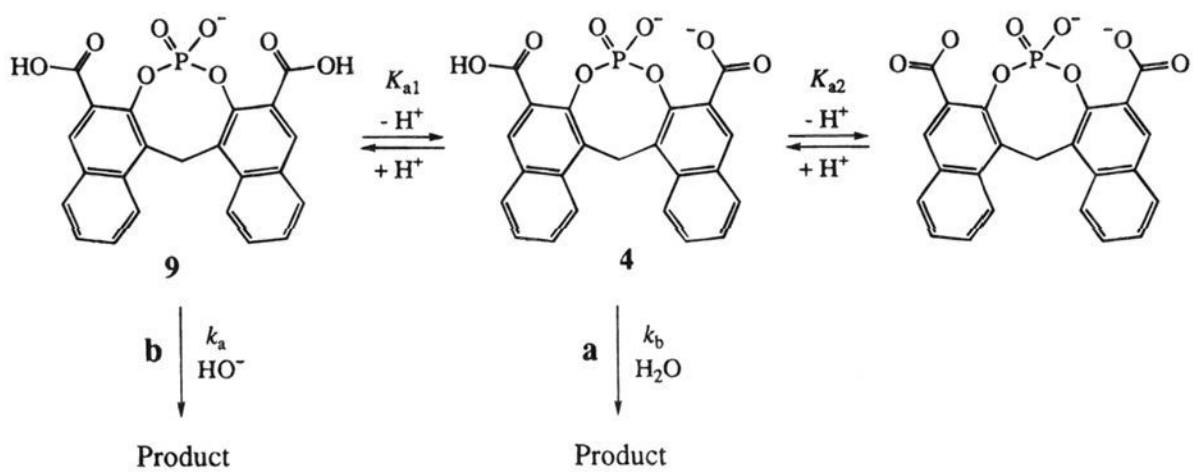

(3-hydroxy-2-naphthoic acid) and its anions. A comparison of the plots of log $k_{obsd}^{H_2O}$ and log $k_{obsd}^{D_2O}$ vs pH(D) is provided in Figure 3. The experimental points were fit to eq 2 (standard error = 3.2×10^{-2}) using the values of $k_p^{D_2O}$, $K_{a1}^{D_2O}$, and $K_{a2}^{D_2O}$ provided in Table 2. The ratio of $k_p^{H_2O}/k_p^{D_2O}$ is 1.9.

Effect of the buffer concentrations on the rate of hydrolysis of 4 was determined by varying the total buffer concentration over a 10-fold range (data not shown) at constant pH values. The pseudo-first-order rate constants (k_{obsd}) were found to be insensitive to changes in the concentrations of the buffers employed {H_3O^+/H_2O, HCO_2H/HCO_2^-, $CH_3CO_2H/CH_3CO_2^-$, $(CH_3)_2As(O)OH/(CH_3)_2As(O)O^-$, $(HOCH_2)_3CNH_3^+/(HOCH_2)_3CNH_2$; see Experimental Section}, indicating that the hydrolysis of **4** is not catalyzed by these buffers.

Temperature dependence of the rate constants for the hydrolysis of 4 was determined at 30, 40, and 50 °C at pH 3.7. Activation parameters were determined from an Arrhenius plot of ln k_{obsd} *vs* K^{-1} (Figure 4) and Arrhenius and Eyring equations.[21] The computed entropy of activation ($\Delta S^{\ddagger}$) and enthalpy of activation ($\Delta H^{\ddagger}$) for the reaction were −3.9 eu and 21.8 kcal mol^{-1}, respectively. No corrections for change of pK_a values of substrate with temperature were required due to the low heats of ionization for carboxylic acids.

(21) Lowry, T. H.; Richardson, K. S. *Mechanism and Theory in Organic Chemistry*, 3rd ed.; Harper & Row Publishers: New York; p 203 and 209.

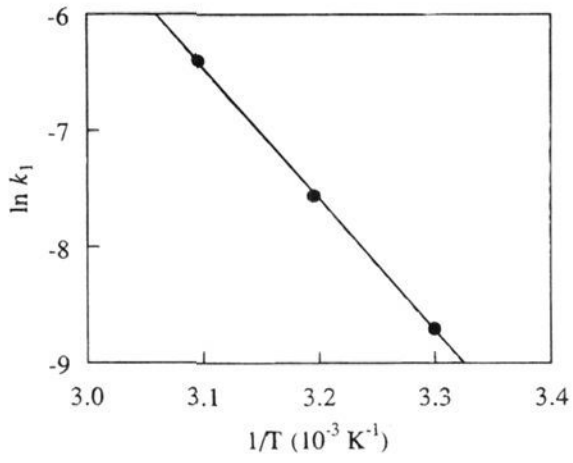

Figure 4. Temperature dependence of the pseudo-first-order rate constants (k_{obsd}) for the hydrolysis of **4** determined at 30, 40, and 50 °C at pH 3.7.

Effect of metal ions on the hydrolysis of 4 was investigated at 50 °C (μ = 1.0 with KCl) under the same conditions as employed in the absence of metal ions. All buffer solutions were passed through Chelex columns to remove trace metal ions. Also, the values of k_{obsd} remained unchanged when determined in the presence and absence of 10^{-3} M EDTA. Exploratory kinetic studies were carried out using 1×10^{-3} M aqueous solutions of $NiCl_2$ and $CoCl_2$ at pH 4.8. These divalent metal

ions were found to have no influence on the values of k_{obsd} for the hydrolysis of **4**.

pH Dependence of the Hydrolysis of 5. Reaction were followed to only *ca.* 10% completion due to the exceedingly slow hydrolysis of this ester. Pseudo-first-order rate constants (k_{obsd}) were determined by the method of initial rates (eq 3,

$$k_{obsd} = \frac{k_{init}}{[R]\epsilon_P} \tag{3}$$

where k_{init} = slope of absorbance *vs* time, [R] = concentration of substrate, and ϵ_P = molar extinction coefficient of product 3-carboxy-2,2′-dihydroxydiphenylmethane and its anions measured at each pH at 300 nm). Included in Figure 3 is a plot of the values of the log of the pseudo-first-order rate constants (k_{obsd}) *vs* pH for the hydrolysis of **5** at 50 °C (μ = 1.0 with KCl). Examination of Figure 3 shows that log k_{obsd} is independent of pH in the pH range examined. The pK_a of the *o*-carboxy group of **5** was determined by spectrophotometric titration. Plots of absorbance at two wavelengths (286 and 244 nm) *vs* pH were computer least-squares fit to a theoretical equation for one pK_a. The determined K_a value for **5** is included in Table 2.

Hydrolysis of 6 was examined at 11 pH values between pH 2 and 8. No hydrolysis of **6** could be detected after 6 months at 50 °C at any of the pH values.

Discussion

The anions of simple phosphate diesters {RO−P(O_2^-)−OR′} are exceedingly stable toward hydrolysis. The rate constant for the hydrolysis of diphenyl phosphate is estimated to be *ca.* 1.2 × 10^{-10} s^{-1} at 100 °C, corresponding to a half-life of nearly 180 years.[22] Assuming that a 10 °C decrease in temperature will decrease the rate constant by half, the estimated rate constant for diphenyl phosphate hydrolysis at 50 °C would be *ca.* 4 × 10^{-12} s^{-1}. Phosphate diesters **4**, **5**, and **6** may be looked upon as diphenyl phosphates in which the two phenyl substituents have been -CH_2- bridged at the *ortho* positions. The unsubstituted **6** may be considered equivalent to diphenyl phosphate in its resistance to hydrolysis. Comparing the rate constants for hydrolysis of diphenyl phosphate with **5** {6.3 × 10^{-8} s^{-1} at 50 °C} shows that the *o*-carboxy group of the latter increases the rate constant by 10^4. Introduction of the second *o*-carboxy group to provide **4** dramatically increases the rate constant for hydrolysis to 1.8 × 10^{-3} s^{-1} at 50 °C. The associated rate enhancement is estimated to be *ca.* 10^8−10^9 over diphenyl phosphate and *ca.* 10^4 over **5**. What follows is a discussion of the mechanisms of hydrolysis of these esters.

The HPLC and ^{31}P NMR experiments show two intermediates to be formed in the hydrolysis of **4** to pamoic acid. The first intermediate ^{31}P NMR spectrum exhibits a chemical shift of −11.18 ppm, 2.73 ppm to lower frequencies from that of the phosphodiester **4**. The structure of this intermediate has been assigned as the cyclic acyl, six-membered-ring phosphate (**7** of Scheme 1). This assignment is in accord with the proposed formation of cyclic acyl salicyl phosphate in the hydrolysis of 2-carboxyphenyl phenyl phosphate and of the 3-nitrophenyl ester of 2-carboxyphenyl phenyl phosphate.[8] In the previous paper in this journal we describe the observation of the formation of such an intermediate in the hydrolysis of bis(2-carboxyphenyl) phosphate.[3]

The ^{18}O isotopic effect on the ^{31}P chemical shift shows (Figure 1) that there are three ^{18}O oxygens incorporated into the H_3PO_4 product when the hydrolysis was performed in 50% (v/v) ^{18}O water and 30% D_2O. The existence of three ^{31}P peaks separated by *ca.* 0.02 ppm accounts for the incorporation of two ^{18}O atoms in the final hydrolysis product of **4**. Considering that the intermediate cyclic acyl phosphate forms *via* intramolecular *o*-CO_2^- attack on phosphorus, the hydrolysis of this intermediate must involve the attack of water, *i.e.*, $H_2O/H_2{}^{18}O$, on phosphorus as well (Scheme 1). This is consistent with the first shift to lower frequencies (0.023 ppm) of the ^{31}P peak. The second ^{18}O incorporation in H_3PO_4 comes from the hydrolysis of **8** and is shown by an extra 0.015 ppm ^{31}P signal (to lower frequencies) shift. The proposed mechanism (Scheme 1) is in accord with no ^{18}O incorporation on the carbonyl carbon and two ^{18}O incorporations on the H_3PO_4 phosphorus.

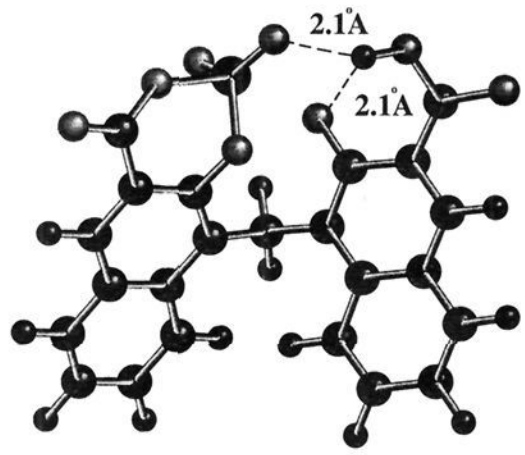

Figure 5. Ball and stick model of **7** showing the bifurcated hydrogen bonding between the free OH group and both the phosphate and carboxyl (*ortho* to the OH group) oxygens.

The question arises as to why does the attack of water occur on phosphorus in the hydrolysis of the cyclic acyl phosphate **7**, rather than on the acylic carbon. Nucleophilic attack on both the carbonyl carbon and P of the five-membered ring of the cyclic enoyl acyl phosphate of pyruvate occurs.[23] Apparently ^{18}O incorporation into six-membered cyclic acyl phosphates has not been previously investigated. The rate of hydrolysis of **7** is comparable to that for the salicyloyl cyclic phosphate **2** (39 °C), k =1.8 × 10^{-5} s^{-1} (pH 5.50) *vs* k = 4.7 × 10^{-5} s^{-1} (pH 5.68),[8] respectively. Due to the stereochemistry of the two naphthalene rings the free OH group of **7** participates in a bifurcated hydrogen bonding with both phosphate and carboxylate (*ortho* to the OH group) oxygens (Figure 5).

Formation of the tetrahedral intermediate that would arise by HO^- attack on the acyl carbonyl of **7** is sterically hindered by the bridged naphthalene ring (Figure 5). Also, hydrogen bonding of the *o*-COOH group to the phosphate oxygen partially quenches the charge on the -(PO_2^-)- moiety of **7** which facilitates HO^- attack on phosphorus. It is well established that such hydrogen bonding as well as metal ligation and increase in ionic strength facilitates phosphate ester hydrolysis by quenching the charges on the phosphate oxygens.[2,5]

The pH dependence of the pseudo-first-order rate constant (k_{obsd}) for the hydrolysis of **4** in water is shown in Figure 3. The line correlating the data points was generated from eq 2 using the derived constants reported in Table 2. The "bell-shaped" pH *vs* log k_{obsd} profile is confined between the pK_a's of the two *ortho* carboxylic groups with the maximum hydrolytic rate being *ca.* midway between the two values. Two kinetically equivalent mechanisms may be written {Scheme 2}. Pathway **a** involves a spontaneous reaction {or one involving water as a reactant} of the ionic species **4** having one *o*-carboxy group ionized and the other un-ionized. The appropriate kinetic

(22) Kirby, A. J.; Younas, M. *J. Chem. Soc. B* **1970**, 510.

(23) O'Neal, C. C.; Bild. G. C.; Smith, L. T. *Biochemistry* **1983**, *22*, 611.

(24) Westheimer, F. H. *Chem . Rev.* **1961**, *61*, 265.

expression is given in eq 4. Pathway **b** involves the reaction

$$k_{obsd} = k_a\left\{\frac{K_{a1}a_H}{K_{a1}K_{a2} + K_{a1}a_H + a_H{}^2}\right\} \quad (4)$$

of HO^- with the ionic species of **4** in which both *o*-carboxy groups are undissociated (**9**; eq 5; K_W equals the autoprotolysis

$$k_{obsd} = \frac{k_b K_W}{K_{a1}}\left\{\frac{K_{a1}a_H}{K_{a1}K_{a2} + K_{a1}a_H + a_H{}^2}\right\} \quad (5)$$

constant of water). The bimolecular rate constant necessary to account for the observed rate by the mechanism of pathway **b** is estimated to be *ca.* 10^7 M^{-1} s^{-1} $\{= k_b = k_a K_{a1}/K_W\}$. This value for k_b is *ca.* 10^{13} times greater than the estimated rate constant for reaction of HO^- with bis(3-nitrophenyl) phosphate (*ca.* 3×10^{-6} M^{-1} s^{-1} at 50 °C; calculated from the value of *ca.* 10^{-4} M^{-1} s^{-1} reported at 100 °C),[22] which in turn exceeds the corresponding rate constant for diphenyl phosphate. Thus, the mechanism of pathway **b** can make no contribution to the hydrolysis of **4**. Also, since the hydrolysis of **4** occurs *via* a cyclic acyl phosphate intermediate (**7**, Scheme 1) the involved pathway **a** must involve a nucleophilic attack of the *o*-CO_2^- on phosphorus rather than a *o*-CO_2^- assisted general base catalyzed attack of water. The deuterium solvent kinetic isotope effect calculated for the reaction of path **a** $\{k_p^{H_2O}/k_p^{D_2O} = 1.9\}$ is at the borderline between KSI values for nucleophilic catalysis and general base catalysis[25] while the computed entropy of activation ($\Delta S^{\ddagger}$) of −3.9 eu is as expected for a monomolecular reaction.

The ground state distance between the participating *o*-CO_2^- oxygen and phosphate P in the minimized structure[3] of **4** is 3.7 Å. Thus, distancewise **4** would appear ideal for a general base catalyzed attack of water as shown in **10**. That this is not the case suggests that such a mechanism is energetically unfavorable. There are no known chemical models for the hydrolysis of phosphodiesters involving general base catalysis of attack of water. General buffer catalysis of H_2O attack is not seen in the hydrolysis of **4** as would be anticipated since there is an absence of neighboring *o*-CO_2^- group general catalysis of H_2O attack (**10**).[14]

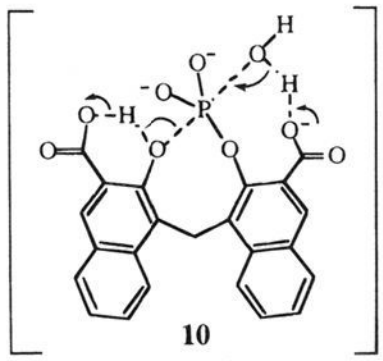

10

The unique roles of both *o*-CO_2^- and *o*-CO_2H functionalities in the hydrolysis of **4** cannot be questioned. In the transition state, the extent of formation of the carboxylate to phosphorus bond and rupture of the phosphorus to leaving oxygen bond remains unknown.[26] The structure of **4** is too big for convenient *ab initio* computations of the desired reaction coordinate which of course would be in the gas phase. The *o*-CO_2^- functionality undoubtedly acts as an intramolecular nucleophile. The role of the *o*-CO_2H must be that of a general acid. If the rate-determining step is the formation of a pentacoordinate species {which need not be a discrete intermediate[25,27] }, the catalytic role of the *o*-CO_2H substituent in the critical transition state cannot be to assist departure of the leaving group. The *o*-CO_2H can only play a catalytic role by increasing the electronegativity of P through hydrogen bonding to the -(PO_2^-)- oxygen. Such a transition state with early attack of *o*-CO_2^- might resemble structure **11** (Figure 6). The hydrogen bonding to the partially negative oxygens of -(PO_2^-)-, as seen in **11**, would explain the role of the *o*-CO_2H if departure of the leaving group had scarcely begun, regardless of the progress of the *o*-CO_2^- attack on P. Cancelation of the negative charge of the -(PO_2^-)- moiety by protonation or ligation has been predicted[28,29] {and shown[5]} to increase the rate constant for nucleophilic attack on phosphorus by $>10^4$. If, however, departure of the leaving group is rate controlling and the

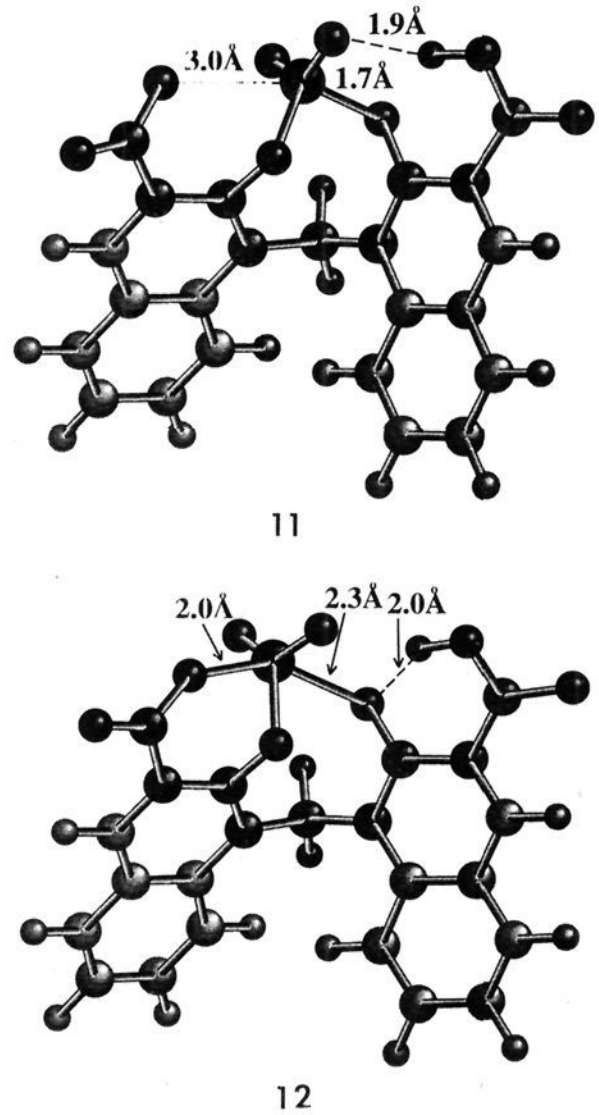

Figure 6. Ball and stick model of **11** and **12** taken from an AM1-derived reaction coordinate trajectory. They show the two types of *o*-CO_2H hydrogen bonding in plausible transition states and, also, show the restriction of total distance between the attacking and leaving oxygens *via* P.

(25) Uchimaru, T.; Tanabe, K.; Nishikawa, S.; Taira, K. *J. Am. Chem. Soc.* **1991**, *113*, 4351.

(26) The *o*-COOH substituent is electron withdrawing such that it stabilizes the developing charge on the leaving oxygen. Ideally one would want to bring this into consideration in the calculation of the rate enhancement due to general acid catalysis by the *o*-COOH substituent. We have not attempted to do so because the σ for *o*-COOH and *o*-COO^- substituents, in the present system are about *ca.* +0.8 and −0.8 and the electronic effect of the carboxyl group will depend on the position of the transition state (vide infra) which dictates the length of the *o*-COO- - -H bond. As stated, we do not know the position of the transition state. We estimate an electronic effect can contribute to the $>10^4$ enhancement in rate no more than 10^2 for a very early transition state and not at all for a late transition state.

(27) Dejaegere, A.; Lom, C.; Karplus, M. *J. Am. Chem. Soc.* **1991**, *113*, 4353.

(28) Westheimer, F. H. In *Phosphorous Chemistry, Developments in American Science*; Walsh, E. N., Griffith, E. J., Parry, R. W., Quin, L. D., Eds.; ACS Symposium Series; American Chemical Society: Washington, DC, 1992.

(29) Dalby, K. N.; Holifelder, F.; Kirby, A. J. *J. Chem. Soc., Chem Commun.* **1992**, 1770.

Scheme 3

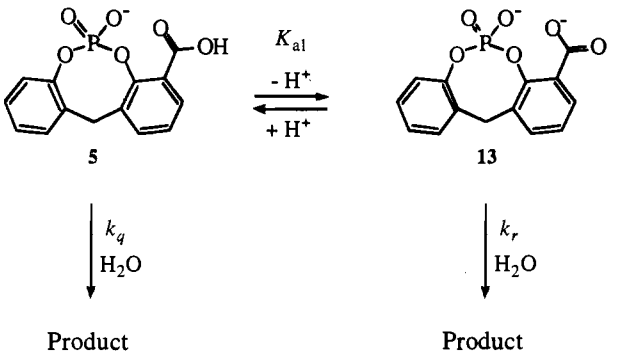

$$-\frac{d[\mathbf{5H}_{total}]}{dt} = k_q[\mathbf{5}] + k_r[\mathbf{13}] \quad (6)$$

$$k_{obsd} = k_q\left\{\frac{a_H}{K_a + a_H}\right\} + k_r\left\{\frac{K_a}{K_a + a_H}\right\} \quad (7)$$

transition state is characterized by almost complete formation of the carboxylate phosphorus bond, the hydrogen bonding of the *o*-CO_2H would have transferred from the -(PO_2^-)- oxygens to the oxygen of the leaving group as shown in **12** (Figure 6).

The pH dependence of the pseudo-first-order rate constant for the spontaneous hydrolysis of **5** is included in Figure 3. As can be seen from Figure 3, values of log k_{obsd} are pH independent. Such a flat profile might suggest that hydrolysis of **5** occurs by intramolecular participation of the *o*-carboxy group in both un-ionized and ionized states as shown in Scheme 3 (eq 7). If the rate constants for the reactions involving *o*-CO_2H (k_q) and *o*-CO_2^- (k_r) participation were comparable, the observed *pseudo*-first-order rate constant for hydrolysis (k_{obsd}) would exhibit no dependence upon pH. This unusual situation has been observed previously by Thanassi and Bruice in a study of the *o*-CO_2H and *o*-CO_2^- group participation in the hydrolysis of phthalic acid monoesters.[30] Discussion of plausible mechanisms for the hydrolysis of **5** is limited by the fact that the rate constants for reaction are so small (*ca.* 10^{-8} s^{-1}) that reactions could be followed to no more than 10% completion in several weeks and accurate deuterium kinetic solvent isotope effects and buffer catalytic coefficients could not be determined. Perhaps the catalytic effect of the *o*-CO_2^- is matched by the electron-withdrawing effect on the leaving group when this substituent is protonated.

Conclusions

The ionic species of the phosphodiester **4** {4,4-methylenebis-(3-hydroxy-2-naphthyl) phosphate} with one *ortho*-carboxylic acid ionized and the other not has been found to hydrolyze with a rate constant 10^9 greater than the estimated rate constant for hydrolysis of diphenyl phosphate. That both *o*-CO_2^- and *o*-CO_2H functions are involved in the catalysis of the rate-limiting step is shown by the observation that the rate constant for the hydrolysis of this anionic species exceeds that for the hydrolysis of a phosphodiester with only one *o*-carboxy function {3-carboxy-2,2′-dihydroxydiphenylmethane, **5**} by 10^4. The pseudo-first-order rate constants for the hydrolysis of **5** are insensitive to pH.

The existence of an intermediate cyclic acyl phosphate in the hydrolysis of **4** was established by ^{31}P NMR and HPLC. The two ^{18}O atom incorporations in the H_3PO_4 reaction product is consistent with intramolecular *o*-CO_2^- nucleophylic attack on phosphorus to provide an acyl phosphate intermediate which undergoes hydrolytic cleavage by $H^{18}O^-$ attack on phosphorus to provide phosphate monoester which undergoes in turn hydrolysis with $H^{18}O^-$ attack on phosphorus. Also, the pH *vs* log k_{obsd} profile, the values of the deuterium solvent kinetic isotope effect, and the activation entropy support a mechanism of hydrolysis of **4** which involves intramolecular attack of *o*-CO_2^- on the phosphate phosphorus assisted by *o*-CO_2H general acid catalysis.

Experimental Section

Materials. Deionized, doubly distilled water was used for all experiments. 4,4′-Methylene(3-hydroxy-2-naphthoic acid), bis(2-hydroxyphenyl)methane, $POCl_3$, and PCl_5 were purchased from Aldrich Chemical Co. 5-Bromosalicylic acid and 3,5-dibromo-2-hydroxybenzyl bromide were from Tokyo Kasei Kogyo Co., Ltd. All the buffer and salt solutions were prepared from reagent-grade chemicals and passed through a Chelex 100 (BioRad) column to remove possible heavy metal contaminants.

Phosphodiester of 4,4′-methylenebis(3-hydroxy-2-naphthoic acid) (4), was prepared by adding $POCl_3$ (1.78 g, 11.6 mmol) to a well stirred mixture of 4,4′-methylenebis(3-hydroxy-2-naphthoic acid) (2.25 g, 5.79 mmol) and PCl_5 (2.65 g, 12.7 mmol) under an argon atmosphere. The mixture was then heated at 100 °C for 4 h, allowed to cool to room temperature, and stirred overnight. Water was then added to the mixture with cooling, and the solid was collected by filtration and dried under reduced pressure. Recrystallization from DMF/acetone provided a yellowish white solid. Spectral analysis showed the following. HR-MS (FAB): calcd for $C_{23}H_{15}O_8P$ $(M + H)^+$ 451.0583, found 451.0597. ^1H NMR (DMSO-d_6): δ ppm 8.32 (d, 2H, J = 8.6 Hz); 8.28 (s, 2H); 8.05 (d, 2H, J = 8.1 Hz); 7.65 (t, 2H, J = 7.6 Hz); 7.52 (t, 2H, J = 7.5 Hz); 4.94 (s, 2H). ^{13}C NMR (DMSO): δ ppm 166.8; 146.7 (d, J_{C-P} = 8.6 Hz, phenolic carbons); 133.5; 130.5; 129.8; 129.7; 128.7; 125.9 (d, J_{C-P} = 2.2 Hz); 125.7 (d, J_{C-P} = 4.0 Hz); 125.6; 123.3; 23.8.

3-Carboxy-2,2′-dihydroxydiphenylmethane was prepared by the method of Finn *et al.*[31] with some modifications. 3,5-Dibromo-2-hydroxybenzyl bromide (26.9 g, 78 mmol) and 5-bromomethyl salicylate (39.0 g, 169 mmol) were combined with 3.9 g of concentrated sulfuric acid and heated under argon at 140 °C with rapid stirring. After 5 h the mixture was allowed to cool to room temperature. Water was then added, followed by neutralization with calcium carbonate (16 g). After steam distillation the residual solid was extracted with acetone, filtered, and evaporated to dryness. Recrystallization from methanol provided crystalline 3′,5′,5-tribromo-2,2′-dihydroxy-3-(methoxycarbonyl)diphenylmethane, mp 184 °C. Spectral analysis showed the following. MS(EI): calcd for $C_{14}H_9O_4Br_3$ (M^+) 492, 494, 496, 498 (1:3:3:1), found 492, 494, 496, 498 (1:3:3:1). ^1H NMR (CD_3OD): δ ppm 7.82 (d, 1H, J = 2.5 Hz); 7.47 (d, 1H, J = 2.5 Hz); 7.38 (d, 1H, J = 2.5 Hz); 7.19 (d, 1H, J = 2.5 Hz); 5.46 (s, 2H); 3.85 (s, 3H).

3′,5′,5-Tribromo-2,2′-dihydroxy-3-(methoxycarbonyl)diphenylmethane (2.84 g, 5.9 mmol) was hydrolyzed by boiling with 10% NaOH (15 mL) for 30 min to provide 3′,5′,5-tribromo-3-carboxy-2,2′-dihydroxydiphenylmethane. The solution was allowed to cool to room temperature, and a nickel–aluminum alloy (50:50, 2.9 g) was added periodically during 4 h along with 10% NaOH (~3 mL). The mixture was filtered and acidified with concd. HCl (pH ~1) to provide the crystalline 3-carboxy-2,2′-dihydroxydiphenylmethane, mp 160 °C. Spectral analysis showed the following. MS(EI): calcd for $C_{14}H_{12}O_4$ (M^+) 244.3, found 244.6. ^1H NMR (CD_3OD): δ ppm, 7.70 (dd, 1H, J = 7.5 Hz and 1.5 Hz); 7.20 (d, 1H, J = 7.5 Hz); 7.03 (d, 1H, J = 1.5 Hz); 7.00 (d, 1H, J = 7.5 Hz); 6.74 (m, 3H); 3.93 (s, 2H).

Phosphodiester of 3-carboxy-2,2′-dihydroxydiphenylmethane (5) was prepared by reacting 3-carboxy-2,2′-dihydroxydiphenylmethane (1.0 g, 4.1 mmol) with a mixture of $POCl_3$ (1.3 g, 8.2 mmol) and PCl_5 (1.9 g, 9.0 mmol) under an argon atmosphere. After heating at 100 °C for 4 h, the reaction mixture was allowed to cool to room temperature and stirred overnight. Water was added with cooling, and the solid

(30) Thanassi, J. W.; Bruice, T. C. *J. Am. Chem. Soc.* **1966**, *88*, 747.

(31) Finn, S. R.; James, J. W.; Standen, C. J. S. *J. Appl. Chem.* **1954**, *4*, 296.

was filtered and dried under reduced pressure. Recrystallization from acetone/diethyl ether provided a pinkish white solid. Spectral analysis showed the following. HR-MS (FAB): calcd for $C_{14}H_{11}O_6P$ $(M + H)^+$ 307.0371, found 307.0380. ^1H NMR (DMSO-d_6): δ ppm 7.68 (d, 1H, $J = 7.0$ Hz); 7.57 (d, 1H, $J = 7.5$ Hz); 7.48 (d, 1H, $J = 7.5$ Hz); 7.17 (q, 2H); 7.08 (t, 1H, 7.0 Hz); 6.97 (d, 1H, $J = 7.5$ Hz); 4.03 (s, 2H).

Phosphodiester of bis(2-hydroxyphenyl)methane (6) was prepared by combining $POCl_3$ (117 μL, 1.25 mmol) with bis(2-hydroxyphenyl)-methane (0.5 g, 2.5 mmol) in pyridine (0.6 mL) and acetonitrile (7 mL) at 0 °C. After stirring for 45 min, water (45 mL) was added to the reaction mixture to provide an oily residue. After decanting the water, the oily residue was dried under reduced pressure. Recrystallization from DMF/acetone provided a white solid. Spectral analysis showed the following. HR-MS (FAB): calcd for $C_{13}H_{11}O_4P$ $(M + H)^+$ 263.0473, found 263.0489. ^1H NMR (DMSO-d_6): δ ppm 7.44 (d, 2H, $J = 7.5$ Hz); 7.15 (t, 2H, $J = 7.5$ Hz); 7.05 (t, 2H, $J = 7.5$ Hz); 6.96 (d, 2H, $J = 7.5$ Hz); 3.97 (s, 2H).

Kinetic Measurements. All kinetic determinations were performed at an ionic strength of 1.0 (with KCl) and a temperature of 50 °C. Buffers employed were HCl (pH 1.0 to 2.5), formate (pH 2.5 to 4.5), acetate (pH 4.5 to 5.5), cacodylate (pH 5.5 to 6.7), and tris-(hydroxymethyl)aminomethane (Tris, pH 7.0 to 9.0). The kinetic runs in D_2O (99.8%, Aldrich) were carried out under the same conditions described for H_2O. Stock solutions of reagents were prepared by first exchanging exchangeable protium with D_2O. The value of pD was obtained by adding 0.29 to the observed pH of solutions in D_2O.[32] The amine/amine hydrochloride buffer solutions were prepared just prior to use by addition of standardized KOH to an aqueous solution of the amine hydrochloride. A minimum of four serially diluted buffer solutions (5.0 to 100.0 mM in total amine) were employed and the pH values of serial dilutions agreed within 0.02 pH unit. Reactions followed by UV−vis absorption measurements were conducted with either a Perkin-Elmer 553 spectrophotometer or a Cary-14 spectrophotometer interfaced to a Zenith computer equipped with OLIS (On-Line Instrument System Inc.) data acquisition and processing software. The cell compartments were thermostated at 50 °C and Spectrocell threaded-top cuvettes with Teflon screwcaps were employed. A Hewlett-Packard 8290 computer was employed for the analysis of the pH−rate profiles and pK_a titrations, with appropriate software programs written for these purposes. pH measurements were carried out with a Radiometer Model M26 pH meter using a combined glass electrode. HPLC kinetic experiments were performed using a reverse phase C18 Altima column (5 μm, 250 mm/4.6 mm) by eluting the reaction mixture (which was thermostated at 40 °C) at room temperature with phosphate buffer pH 4.0/acetonitrile in solvent gradient from 5 to 40% acetonitrile in the first 3 min and constant 40% acetonitrile up to 10 min, at 1.5 mL/min. The signals were followed at 290 and 320 nm on a diode array UV−vis detector. The column was periodically regenerated with methanol−water to prevent clogging. HPLC kinetic data were fitted using the Mathcad 5+ program (Math Soft Inc., Cambridge, MA).

NMR Experiments. Samples were prepared in D_2O/DMSO-d_6 (Isotech) before each experiment. The ^{31}P, ^{13}C, and ^1H NMR spectra were recorded at 202.46, 125.77, and 500.12 MHz, respectively, on a GN-500 instrument at 25 °C. For the ^{31}P NMR data processing a sine bell apodization with a 25-degree shift was used prior to the Fourier transform. ^{31}P spectra were referenced to the signal of external H_3PO_4 and ^{13}C and ^1H spectra to the internal DSS {2,2-dimethyl-2-silapentane-5-sulfonate}. Assignments of the ^{31}P chemical shifts is in agreement with the following rules: (a) the ^{31}P chemical shifts for aliphatic phosphate monoester dianions are $\delta \approx 3$ ppm; monoester monoanions $\delta \approx 0$ ppm; acyclic diester monoanions $\delta \approx -1$ ppm; acyclic diester free acid $\delta \approx -2$ ppm; and six-memberd cyclic esters $\delta \approx -4$ to -14 ppm; (b) an increase of ca. 3° in the O−P−O bond angle of the dianionic phosphate gives 4 ppm upfield shift; (c) charge alone does not appear responsible for the deshielding, because acyclic monoanion and free acid have similar chemical shifts and significantly similar O−P−O bond angles.[9] In the case of ^{18}O isotopic experiments the reaction was run in 20% DMSO-d_6 50% ^{18}O water and 30% D_2O (pH $\approx$ 7). Due to DMSO, intermediate was broad and we could not detect any fine structure of the ^{31}P signal. Phosphoric acid was precipitated with $BaCl_2$, filtered, and released with H_2SO_4. After centrifugation of $BaSO_4$, the clean solution was recorded for ^{31}P spectrum.

Acknowledgment. This work was supported by the Office of Naval Research and the National Institute of Health.

Supporting Information Available: Figure S1, ^{31}P NMR spectrum of the partially hydrolyzed **4**; Figure S2, ^1H NMR in the 4.9−5.2 ppm region of the partially hydrolyzed **4**; Figure S3, normalized UV−vis spectra of **4** and its reaction intermediates and product (3 pages). This material is contained in many libraries on microfiche, immediately follows this article in the microfilm version of the journal, can be ordered from the ACS, and can be downloaded from the Internet; see any current masthead page for ordering information and Internet access instructions.

JA9519694

(32) Fife, T. H.; Bruice, T. C. *J. Phys. Chem.* **1961**, *65*, 1079.